13th World Conference on Earthquake Engineering
Vancouver, B.C., Canada
August 1-6, 2004
Paper No. 1073

PERFORMANCE OF MECHANICAL SPLICES WITHIN THE PLASTIC HINGE REGION OF BEAMS SUBJECT TO CYCLIC LOADING

R. Joseph REETZ[1], Malte von RAMIN[2], Adolfo MATAMOROS[3]

SUMMARY

The experimental response of two beam specimens with mechanical splices within the plastic hinge region subjected to reversed cyclic loading is discussed. Because basic principles dictate that the strain demand in the reinforcement is inversely proportional to the amount of longitudinal reinforcement, the amount of longitudinal reinforcement in the first specimen was set to approximately the minimum allowed by the ACI 318 Code for beams, while the second specimen had twice as much. Strains in the reinforcement and rotation within the plastic hinge were monitored during the tests. A comparison is made between the observed behavior of the splices in the plastic hinge of the beams and that observed in direct tensile tests. Recommendations are made about the use of mechanical splices in plastic hinge regions.

INTRODUCTION

Guidelines for the use of mechanical splices in the 2002 ACI Building Code [1] establish qualification requirements dependent entirely on the strength of the splice. Provisions in the ACI Code establish two different categories of mechanical splices. Mechanical splices able to transfer a minimum of 125 percent of the yield strength of the bar are classified as type 1 splices, and their use is precluded in regions of potential plastic hinging. Type 2 mechanical splices are required to transmit the full tensile strength of the bar, and are the only type of splice that may be used in potential plastic hinge regions.

Although the strength of mechanical splices is an important consideration for seismic design, the maximum strain that can be developed in the plastic hinge region in the mechanical splice-bar assembly prior to fracture is also of great significance. The research conducted was aimed at providing recommendations for a minimum strain demand that mechanical splices should be able to sustain in order to achieve specified rotation or member drift demands prior to failure of the connection.

EXPERIMENTAL PROGRAM

[1] Graduate Assistant, University of Kansas, USA. Email: joereetz@ku.edu
[2] Graduate Assistant, University of Kansas, USA. Email: mvramin@ku.edu
[3] Assistant Professor, University of Kansas, USA. Email: amatamor@ku.edu

The purpose of the experimental research was to investigate the behavior of beam-column connections in which mechanical couplers were used to splice the reinforcing steel. Two specimens were cast and tested. The controlled variables of the study were the dimensions of the cross section and the longitudinal reinforcement ratio.

The specimens were designated according to the differences in the cross section dimensions of the beam. Specimen A1 had a cross section of 12 by 24 inches, while B1 had a cross section of 10 by 16 inches (Fig. 1). Both specimens had concrete compressive strengths of 6000 psi. The longitudinal reinforcement for both specimens consisted of four #7 bars, with reinforcement ratios of 0.47% and 0.92%, respectively. For specimen A1, this corresponded to approximately the minimum amount of reinforcement allowed by the 2002 ACI Building Code [1]. All bars were spliced at the location of the plastic hinge using Lenton® A2 Standard Couplers, which meet the requirements for type 1 splices according to the ACI 318 Code. The location of the couplers was approximately three inches from the interface between the beam and the base block. The amount of transverse reinforcement was proportioned in accordance with Chapter 21 of the 2002 ACI Code [1].

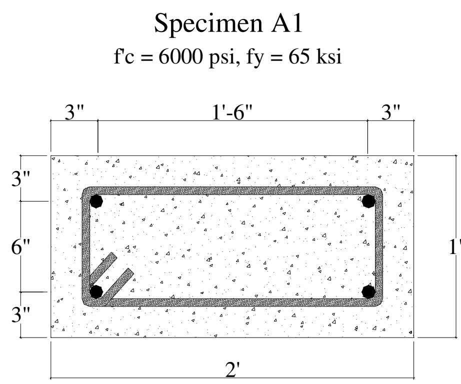

Figure 1.A

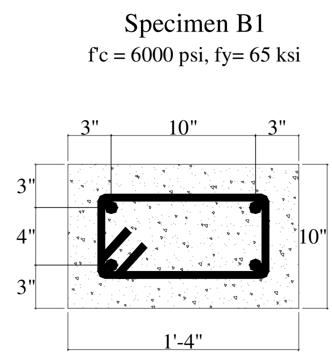

Figure 1.B

Figure 1. Specimen cross-section

The specimens consisted of a large base block and a vertical element extending from the base, representing one half of a beam that is fixed at both support locations (Fig. 1 and 2). The specimens were tested under cyclic loading, with increasing levels of lateral drift, using a hydraulic actuator. A diagram of the test configuration is shown in Fig. 2.

The displacement history for each of the two tests is shown Fig. 3. The load point displacement, rotation in the plastic hinge, rigid body rotation of the entire specimen, and average strain in the reinforcement over the length of the plastic hinge were measured using linear displacement transducers (LVDT's). Rotations were measured using two displacement transducers fixed to the specimen in the proximity of the two layers of longitudinal reinforcement, at a distance d (effective depth of the beam) from the support. In addition strain gages were also used to monitor the strain in the longitudinal reinforcement. The locations of the displacement transducers and strain gages are shown in Fig. 4.

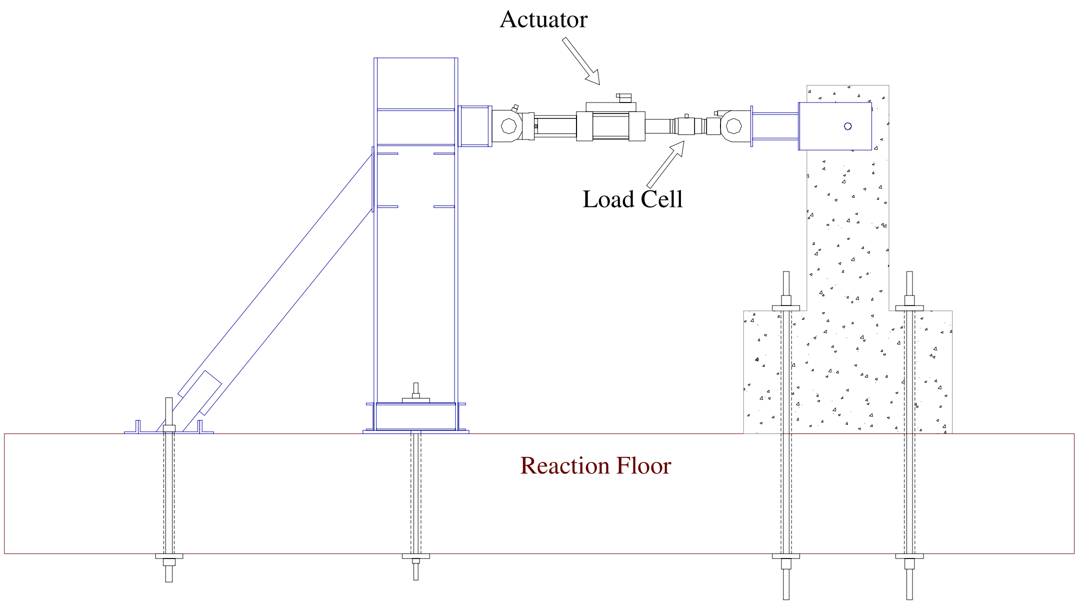

Figure 2. Experimental configuration.

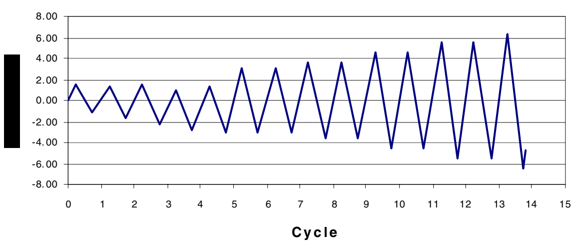

Figure 3.B
Displacement History
Specimen B1

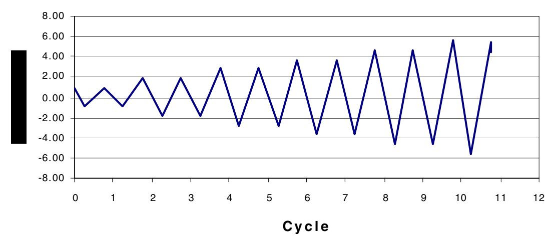

Figure 3.A
Displacement History
Specimen A1

Figure 3. Displacement history for specimens A1 and B1

EXPERIMENTAL RESULTS

Displacement measurements were used to infer force-displacement and moment-rotation relationships for each specimen (Figs. 5-7). These curves show that both specimens reached drift ratios of over 4 percent without a considerable loss in shear capacity. Specimen B1 showed a significant decline in shear strength at a drift ratio of 6 percent, due to buckling of the longitudinal reinforcement. No fracture of the reinforcement at the splice was observed. At the time of failure the specimen exhibited significant damage to the concrete inside the confined core.

The behavior of specimen A1 was similar to that of B1 up to a drift ratio of 5.5 percent. At this point, one of the bars subjected to tension fractured at the interface between the mechanical splice and the bar, immediately below the coupler.

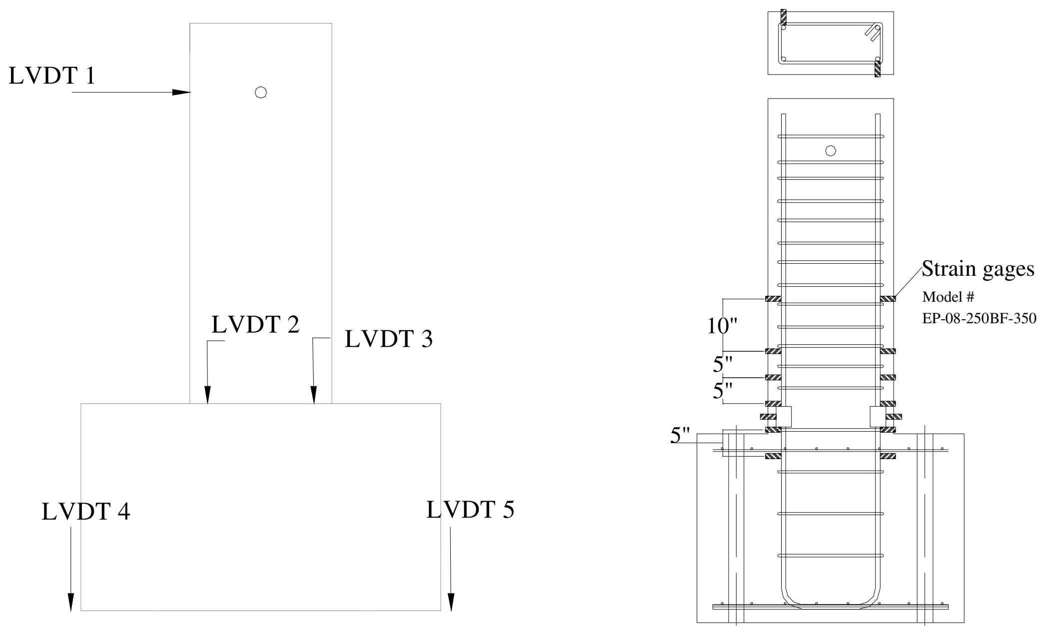

Figure 4. Location of displacement transducers and strain gages

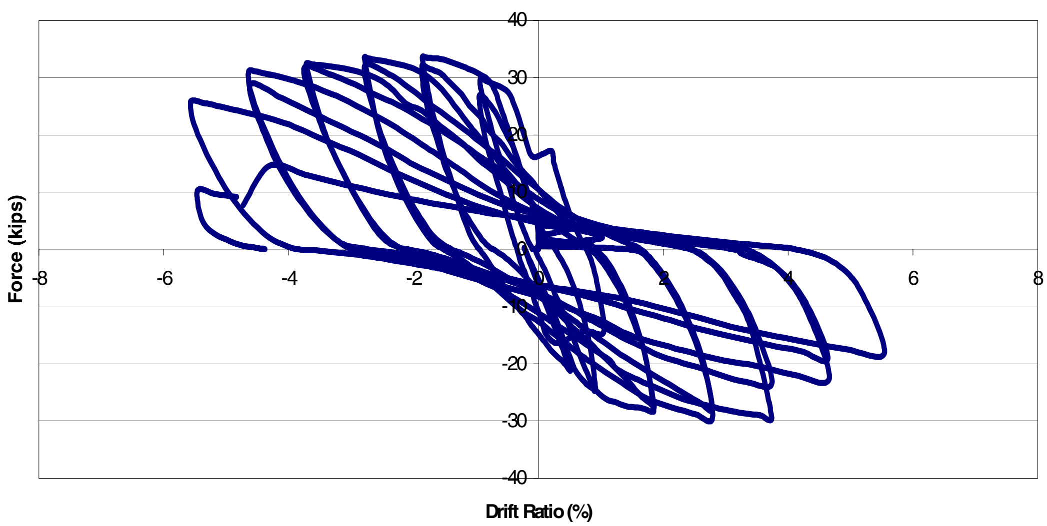

Figure 5. Shear force vs. displacement for specimen A1.

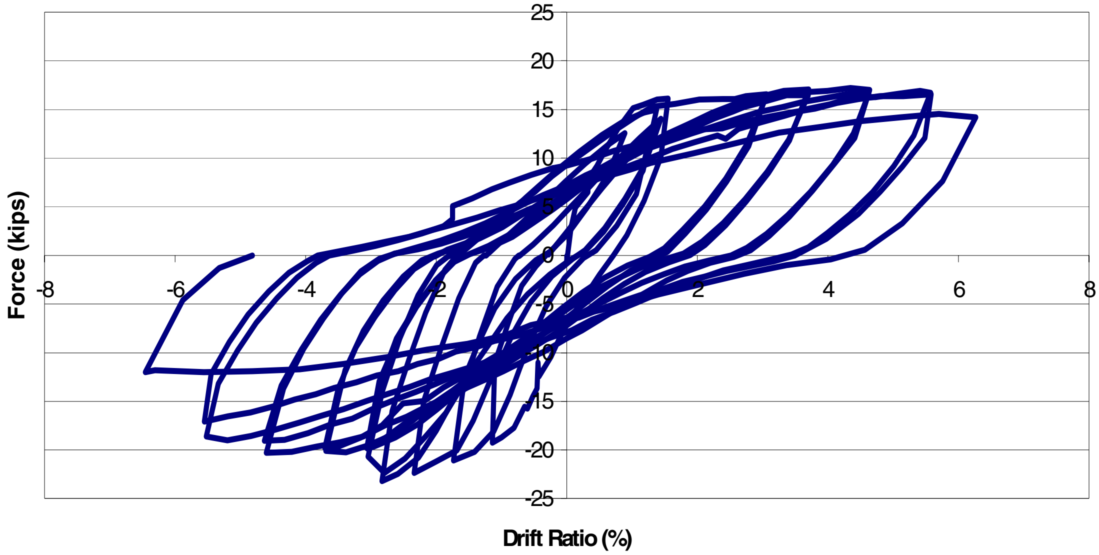

Figure 6. Shear force vs. drift ratio for specimen B1.

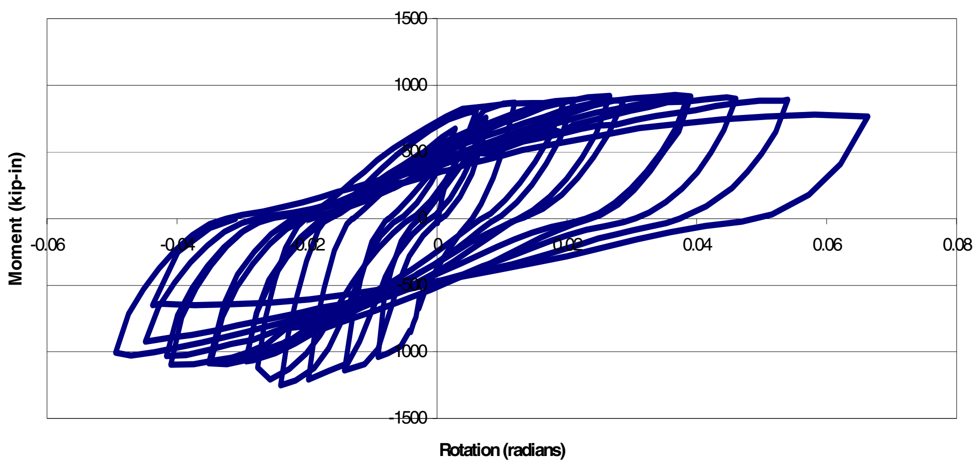

Figure 7. Moment vs. rotation at the plastic hinge region for specimen B1.

RELATIONSHIP BETWEEN STRAIN AND DRIFT

In addition to the aforementioned data, the relationship between the strain in the reinforcement at the plastic hinge and the drift ratio was examined using data from previous tests of beams without couplers. The additional data were obtained from a study at the University of Illinois on drift limits for high-strength concrete columns, Matamoros [2]. The strains in specimens containing couplers were found to be similar to the strains that were measured in beams with plain reinforcement.

An equation was developed to relate the average strain in the reinforcement over the length of the plastic hinge, assumed to be equal to the effective depth of the beam, and the drift ratio. From this relationship recommendations can be made as to the minimum amount of strain a mechanical coupler should be able to withstand before fracture. The equation was derived using the product of curvature and distance from the reinforcing steel to the neutral axis.

Using equilibrium, a relationship was derived to find the distance from the reinforcing steel to the neutral axis. This is illustrated in Fig 8.

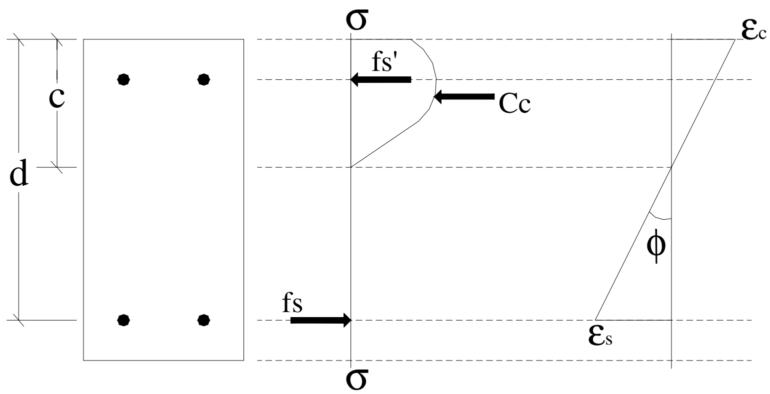

Figure 8. Stress and strain distributions in flexural members

By neglecting the effect of the reinforcing steel in the compression zone, f_s' (Fig. 1), horizontal equilibrium dictates that:

$$P = C_C - F_S \tag{1}$$

where:

$$C_C = 0.85\, f_c^{'}\, a\, b = 0.85\, f_c^{'}\, \beta_1\, c\, b \tag{2}$$

and

$$F_S = A_S\, F_y \tag{3}$$

Substituting Eqs. 2 and 3 into equation 1, and solving for c, the following expression for the neutral axis depth is obtained.

$$c = \frac{1}{0.85 f_c^{'} \beta_1 b}\left(P + A_S F_y\right) = \frac{d}{0.85 f_c^{'} \beta_1}\left(\frac{P}{b\,d} + \rho\, f_y\right) \tag{4}$$

Equation 4 was derived based on the assumption of monotonic loading, and does not reflect the effect of load reversals on the position of the neutral axis. Wight [3] observed in tests of beams and columns under cyclic loading that the neutral axis tended to shift towards the center of the member with increasing damage to the concrete. This effect is due to degradation of the concrete outside of the confined core and plastic deformations in the reinforcement. However, Wight found that this effect was considerably less significant for beams than it was for columns. Based on Eq. 4, the distance from the tensile reinforcement to the neutral axis is given by:

$$d - c = d - \frac{d}{0.85 f_c^{'} \beta_1}\left(\frac{P}{b\,d} + \rho\, f_y\right) = \frac{d}{0.85 \beta_1}\left(0.85\beta_1 - \frac{P}{f_c^{'}\, b\, d} + \frac{\rho\, f_y}{f_c^{'}}\right) \tag{5}$$

In order to establish a relationship between drift and strain demand in the reinforcement, it is necessary to establish a relationship between the lateral drift in the members and the curvature demand in the plastic hinge region. The total curvature in the plastic hinge region is the sum of the curvature at yield and the plastic curvatures (Fig. 9).

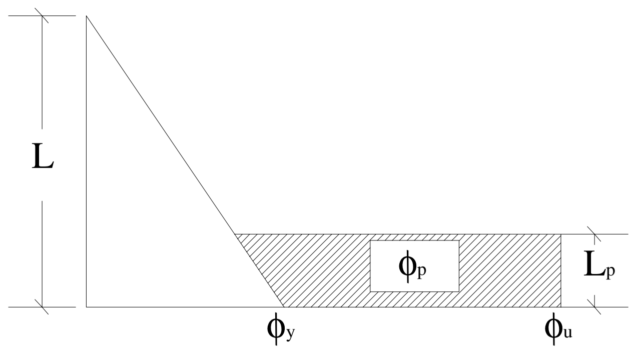

Figure 9. Assumed curvature distribution for drifts greater than yield.

The curvature at yield is given by:

$$\phi_y = \frac{f_y}{E_S\,(1-k)\,d} = \frac{\varepsilon_y}{(1-k)\,d} \tag{6}$$

The plastic deformation was calculated as the total displacement minus the displacement at yield. The displacement at yield was assumed to have two components, one due to flexure and one due to slip of the reinforcement. Deformations related to shear were assumed small in comparison to the first two components. The displacement at yield due to slip is given by:

$$\delta_{y-slip} = \frac{f_y^2 \;\; d_b\, L}{E_S \;\; 4 \;\; u \;\; \left(d-c\right)} \tag{7}$$

Where u is the bond strength. A lower bound to the bond strength was adopted from Moehle and Sozen [4] as:

$$u = 6\sqrt{f_c^{'}} \tag{8}$$

Using Eqs. 7 and 8, the displacement at yield was calculated as:

$$\delta_y = \delta_{y-flexure} + \delta_{y-slip} = \varepsilon_y \left(\frac{L^2}{3(1-k) \;\; d} - \frac{f_y \;\; d_b\, L}{24 \;\; \sqrt{f_c^{'}} \;\; \left(d-c\right)} \right) \tag{9}$$

The plastic displacement was found by subtracting the displacement at yield from the total displacement.

$$\delta_p = \delta - \varepsilon_y \left(\frac{L^2}{3(1-k)\ d} - \frac{f_y\ \ d_b\, L}{24\ \sqrt{f_c^{'}}\ \ (d-c)} \right) \tag{10}$$

The plastic rotation was found by dividing the plastic displacement by the length of the plastic hinge. The length of the plastic hinge was assumed equal to the effective depth. There were two reasons for this assumption. By measuring the average curvature over a longer region the risk of having inelastic deformation outside the control region is minimized. The second reason is that because the purpose is to compare results with tests of mechanical splices done "in air", it is important to monitor a length representative of the size of a specimen used in a monotonic tensile test of a splice. Using a larger plastic hinge length reduces the effect of peak strain values, that occur at flexural cracks, and that are not representative of the average demand in the splice-bar assembly.

$$\theta_p = \delta_p / L_p = \left[\delta - \varepsilon_y \left(\frac{L^2}{3(1-k)\ d} - \frac{f_y\ \ d_b\, L}{24\ \sqrt{f_c^{'}}\ \ (d-c)} \right) \right] \left(\frac{1}{L_p} \right) \tag{11}$$

To obtain the plastic curvature, the plastic rotation must be divided by the distance from the loading point to the center of the plastic hinge.

$$\phi_p = \frac{\theta_p}{\left(L - \frac{L_p}{2} \right)} = \left[\delta - \varepsilon_y \left(\frac{L^2}{3(1-k)\ d} - \frac{f_y\ \ d_b\, L}{24\ \sqrt{f_c^{'}}\ \ (d-c)} \right) \right] \left(\frac{1}{L_p \left(L - \frac{L_p}{2} \right)} \right) \tag{12}$$

The total curvature was obtained by adding Eq. 6 and 12.

$$\phi = \phi_y + \phi_p = \left[\frac{\varepsilon_y}{(1-k)\,d} + \left(\delta - \varepsilon_y \left(\frac{L^2}{3(1-k)\ d} - \frac{f_y\ \ d_b\, L}{24\ \sqrt{f_c^{'}}\ \ (d-c)} \right) \right) \left(\frac{1}{L_p \left(L - \frac{L_p}{2} \right)} \right) \right] \tag{13}$$

Reviewing the strain distribution in Fig. 8, it can be seen that for small angles the strain in the tensile reinforcement is approximately equal to the product of curvature and the distance from the neutral axis. This is reflected by Eq.14, which is shown below.

$$\varepsilon_s = (d-c)\phi \tag{14}$$

$$\varepsilon_s = \frac{d}{0.85\beta_1} \left(0.85\beta_1 - \frac{P}{f_c^{'} b\, d} + \frac{\rho\, f_y}{f_c^{'}} \right) \left[\frac{\varepsilon_y}{(1-k)\,d} + \left(\delta - \varepsilon_y \left(\frac{L^2}{3(1-k)\ d} - \frac{f_y\ \ d_b\, L}{24\ \sqrt{f_c^{'}}\ \ (d-c)} \right) \right) \left(\frac{1}{L_p \left(L - \frac{L_p}{2} \right)} \right) \right]$$

Application of the Equation

In order to calibrate Eq. 14, strain values at various drift ratios were calculated for all specimens with and without mechanical splices. These calculated values were compared with the actual strains measured during the original tests. Data for beams containing plain reinforcing steel came from six specimens tested by Matamoros [2]. These values were compared with the aforementioned specimen, B1, which contained couplers.

A plot showing the ratio of calculated to measured strain versus drift ratio is shown in Fig. 10.

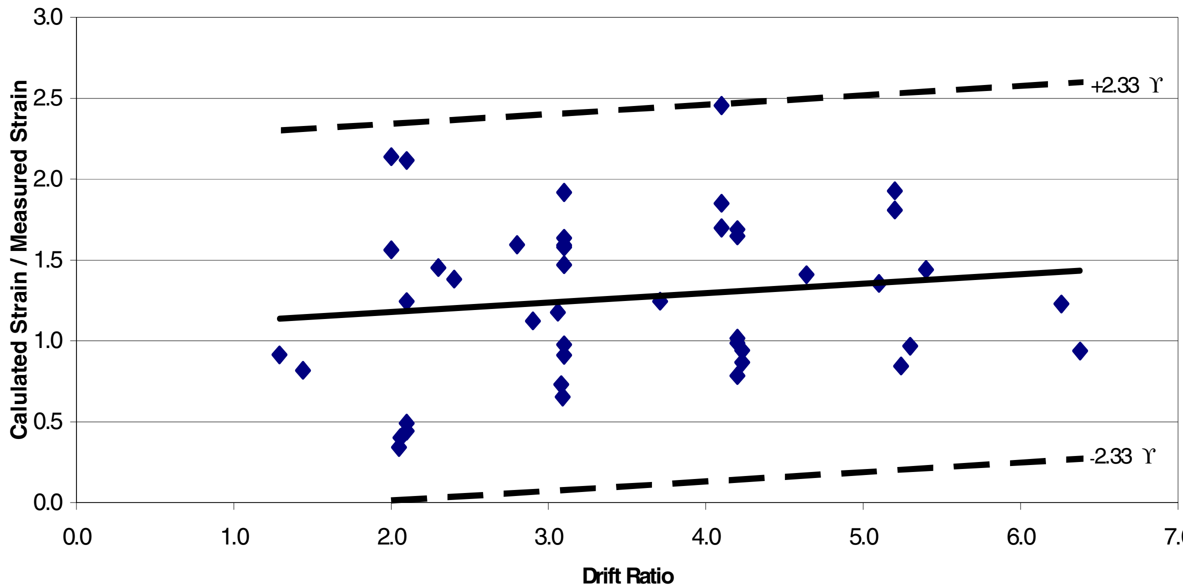

Figure 10. Ratio of calculated to measured strain vs. drift ratio

Figure 10 shows that the ratio was slightly greater than one for drift ratios above 1% and tended to increase with drift ratio. As previously mentioned, this was expected due to the neutral axis shifting towards the center of the cross section due to degradation of the concrete [Wight, 3]. By neglecting this trend a higher factor of safety is provided for members subjected to higher drift ratios. Table 1 shows the parameters for the specimens included in Fig. 11. Table 2 shows the results from a linear regression analysis between calculated and measured values. The average ratio of calculated to measured strain was 1.3 and the standard deviation was 0.5, resulting in a coefficient of variation of approximately 40%.

Table 1

Specimen ID	Number of Data Points	f'_c (psi)	b (in)	h (in)	d (in)	ρ	L (in)
B1	7	6,000	10	16	13	0.9%	54
C10-00	4	10,000	8	8	6.5	1.2%	24
C5-10	2	6,900	8	8	6.25	1.2%	24
C10-05	8	10,100	8	8	6.25	1.2%	24
C5-20	8	7,000	8	8	6.25	1.2%	24
C10-10	6	9,830	8	8	7	1.1%	24
C5-00	9	5,500	8	8	7	1.1%	24

Table 2

Mean	1.27
Standard Deviation	0.50
Slope of the Line	0.06
Y-intercept	1.06
R-squared value	0.02

Figure 11 shows a plot of strain as a function of drift ratio for a specimen without mechanical splices. Figure 12 shows the same plot for a specimen with mechanical couplers in the reinforcement. For both specimens the calculated value provided a good fit for the experimental results, and the curve for the mean plus one standard deviation provided a safe upper bound.

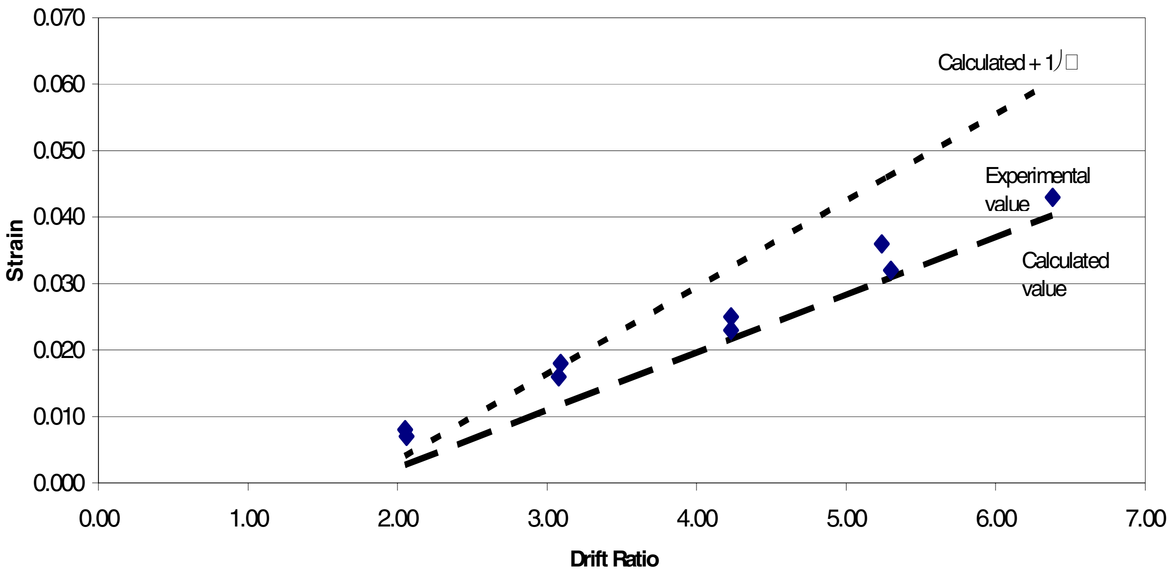

Figure 11. Average strain in the plastic hinge region vs. drift ratio for specimen C5-00 tested by Matamoros [2].

Effect of Reinforcement Ratio and Concrete Compressive Strength on Reinforcement Strain

The strain demand was calculated for various values of concrete compressive strength and reinforcement ratio using Eq. 14. The yield strength of the steel, effective depth, and load-point distance were kept constant at 60,000 psi, 24 inches and 120 inches, respectively. The results are shown in Fig. 13. The strain in the reinforcement increased as the concrete compressive strength increased and the reinforcement ratio decreased. For lower concrete strengths the effect of the reinforcement ratio was more significant. Eq. 14 indicates that for drift ratios on the order of 2%, variations in compressive strength and reinforcement ratio can cause changes up to 100% in the average strain demand in the reinforcement.

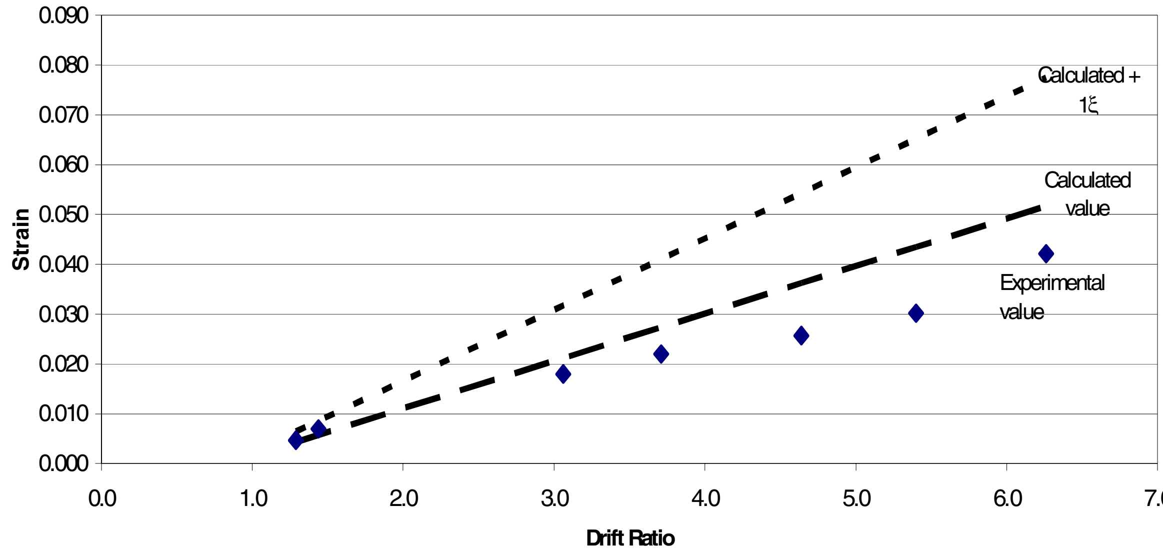

Figure 12. Average strain in the plastic hinge region vs. drift ratio for specimen B1

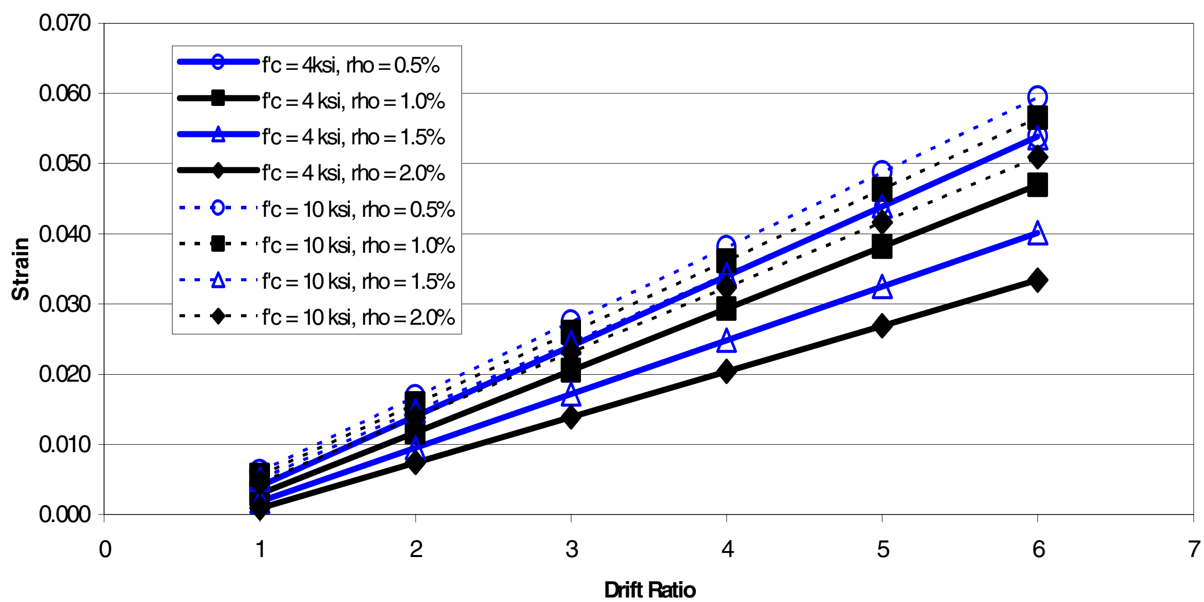

Figure 13. Average strain demand in the plastic hinge vs. drift ratio for a beam with yield strength of 60 ksi, d = 24 in., and L = 120 in.

RECOMMENDATIONS

Building Codes typically limit the maximum interstory drift in a structure, calculated based on the design earthquake, to a maximum of 2%. In order to relate strain and drift ratio in a simpler manner, Eq. 14 can be simplified using conservative assumptions. Values for yield strength (f_y), modulus of elasticity (E_s), concrete compressive strength (f'_c), reinforcement ratio (ρ), the ratio of the neutral axis depth to effective depth of the cracked transformed section (k), bar diameter (d_b), and the ratio of the distance from the support to the inflection point to the effective depth (L/d), were inserted into the following equations to reduce the number of variables. The values used are shown in Table 3. Conservative assumptions were made for the values of yield strength, compressive strength, reinforcement ratio, and the ratio of the neutral axis depth to effective depth of the cracked transformed section.

Table 3

f_y (psi)	Es (psi)	f'$_c$ (psi)	ρ	k	d_b (in)	L/d
60000	29000000	10000	0.3%	0.2	1	5

Equation 5 was evaluated using the assumptions presented in Table 3 to find the distance between the neutral axis and the centroid of the tension reinforcement. Neglecting the term for axial load:

$$d - c = \frac{d}{0.85\beta_1}\left(0.85\beta_1 + \frac{\rho f_y}{f_c^{'}}\right) \tag{15}$$

Substituting the values from Table 3 into Eq. 19:

$$d - c = \frac{d}{0.85 * 0.65}\left(0.85 * 0.65 + \frac{0.003 * 60000}{10000}\right) = 0.95d \tag{16}$$

The curvature and drift ratio can be related by modifying Eq. 10. This is done by replacing the total displacement with the product of drift ratio and length, minus the displacement at yield.

$$\delta_p = D.R.* L - \frac{\left(f_y / E_S\right) L^2}{(1-k)d \;\; 3} - \frac{f_y^2 \, d_b \, L}{E_S \, 24\sqrt{f_c^{'}}\,(d-c)} \tag{17}$$

The curvature can be expressed as:

$$\phi = \left[\frac{f_y / E_S}{(1-k)d} + \left(D.R.* L - \frac{\left(f_y / E_S\right) L^2}{(1-k)d \;\; 3} - \frac{f_y^2 \, d_b \, L}{E_S \, 24\sqrt{f_c^{'}}\,(d-c)}\right)\left(\frac{1}{L_p\left(L - \frac{L_p}{2}\right)}\right)\right] \tag{18}$$

Substituting the values from Table 3 into Eq. 18:

$$\phi = \left[\frac{1}{387\,d} + \left(D.R. - \frac{0.0009L}{d} - \frac{1}{19(d-c)}\right)\left(\frac{L}{L_p\left(L - \frac{L_p}{2}\right)}\right)\right] \tag{19}$$

Setting the length of the plastic hinge equal to the effective depth, the equation becomes:

$$\phi = \left[\frac{1}{387d} + \left(D.R. - \frac{0.0009L}{d} - \frac{1}{19\,(d-c)} \right) \left(\frac{L}{d\left(L - \frac{d}{2}\right)} \right) \right] \tag{20}$$

The product of Eqs. 16 and 20 gives the strain in the reinforcement.

$$\varepsilon_s = 0.95d \left[\frac{1}{387d} + \left(D.R. - \frac{0.0009L}{d} - \frac{1}{19\,(d-c)} \right) \left(\frac{L}{d\left(L - \frac{d}{2}\right)} \right) \right] \tag{21}$$

Using the length to depth ratio from Table 3, Eq. 21 simplifies to:

$$\varepsilon_s = 1.05D.R. - 0.0021 - \frac{1}{17d} \tag{22}$$

For the typical range of values for effective depth, Eq. 22 calculates the percent strain to be less than the drift ratio for drift ratios up to 8%. For this reason, a conservative and simple approach is to assume that the strain in the reinforcement is approximately equal to the drift ratio:

$$\varepsilon_s \approx D.R. \tag{23}$$

Equation 23 provides an estimate of the mean demand expected in the reinforcement for a given drift ratio. Actual strain values measured in beams will vary as shown in Fig. 10, so a safer estimate is desirable for the purpose of design. In order to account for the probability of strain demand being higher than that calculated, a coefficient k is introduced based on the standard deviation observed in the data used to calibrate Eq. 14. Consequently, the average strain demand in the plastic hinge region is approximately given by.

$\varepsilon_s = k * D.R.$ (23)

Table 4 shows the value of k for various probabilities of failure.

Table 4

Probability of Failure	k-value
15%	1.5
5%	2.0
1%	2.25

Recommendation for Minimum Strain Capacity of A Mechanical Splice

Because the failure of mechanically spliced bars is due to brittle fracture of the reinforcement, it is essential that this type of failure be avoided prior to reaching the limiting drift ratio of a structure. Consequently, any recommendation for the minimum acceptable performance of mechanical splices must allow for a very low probability that this type of failure will take place. For limiting drift ratios of two percent, it is suggested that the probability of failure be limited to at least 5%, and preferably to 1%. The data analyzed in this paper indicates that in order to limit the probability of failure the splice must be able to reliably sustain a strain of at least 4.0% prior to fracture of the bar-splice assembly in a tensile test.

The proposed recommendations were consistent with the observed behavior of specimens with mechanical splices tested as part of the experimental program. In both instances, the specimens were able to reach limiting drift ratios that exceeded 5%. The specimen with the minimum amount of reinforcement allowed by the code failed due to fracture of the splice at a drift ratio of 5.5%, while the specimen with twice the minimum amount of reinforcement allowed by the code failed due to buckling of the longitudinal reinforcement without failure of the splice. Recommendations from the manufacturer of the mechanical splices used in the tests indicate that the reliable strain demand is on the order of 4%. The proposed recommendations would limit the use of these devices to members in which drift demands below 2% are expected, which would result in a considerable margin of safety based on the results from the static tests.

Acknowledgments

The authors would like to express their gratitude to Builders Steel from Kansas City Missouri and Erico Products for donating materials used in this study.

REFERENCES

1. ACI Committee 318 (2002). “Building Code Requirements for Structural Concrete (318-02) and Commentary (318R-02)”, Farmington Hills, Michigan.

2. Matamoros, A. (1999). “Study of Drift Limits for High-Strength Concrete Columns”. PhD. Thesis, Department of Civil Engineering, University of Illinois at Urbana-Champaign.

3. Wight J. K., and Sozen, M. A., (1973) “Shear Strength Decay in Reinforced Concrete Columns Subjected to Large Deflection Reversals” Civil Engineering Studies. Structural Research Series No. 403. University of Illinois at Urbana-Champaign, Urbana, Illinois.

4. Sozen, M. A. and Moehle, J. P. (1990) "Development and Lap-Splice Lengths for Deformed Reinforcing Bars in Concrete". Report to The Portland Cement Association and The Concrete Reinforcing Steel Institute, August 1990.